AD-A066 745 TEXAS UNIV AT AUSTIN APPLIED RESEARCH LABS F/G 17/1
MECHANICALLY SIMULATED RDT OF THE AN/SQS-23,(U)
OCT 79 W W RYAN N00024-69-C-1129
UNCLASSIFIED ARL-TM-69-18 NL

1 OF 1
ADA
066745

END
DATE
FILMED
5-79
DDC

APPLIED RESEARCH LABORATORIES

THE UNIVERSITY OF TEXAS AT AUSTIN

ARL-TM-69-18
17 October 1969

Copy No. /

MECHANICALLY SIMULATED RDT OF THE AN/SQS-23

NAVAL SHIP SYSTEMS COMMAND
N00024-69-C-1129
Proj. Ser. No. SF 11121100, Task 8212

William W. Ryan, Jr.

14 ARL-TM-69-18
17 October 1969

6 **MECHANICALLY SIMULATED RDT OF THE AN/SQS-23**

10 William W. Ryan, Jr.

11 17 Oct 79

12 25p.

NAVAL SHIP SYSTEMS COMMAND
15 N00024-69-C-1129
Proj. Ser. No. SF 11121100, Task 8212

16 F11121 17 SF11121100

627 11 N

This document is subject to special export controls and each transmittal to foreign governments or foreign nationals may be made only with prior approval of NAVSHIPS 00V1C

DISTRIBUTION STATEMENT A
Approved for public release;
Distribution Unlimited

APPLIED RESEARCH LABORATORIES
THE UNIVERSITY OF TEXAS AT AUSTIN
AUSTIN, TEXAS 78712

~~For Official Use Only~~

ABSTRACT

This memorandum describes the construction and performance of a device for mechanically simulating the Rotating Directional Transmission (RDT) mode of the AN/SQS-23. Pressure envelopes and frequency functions of the mechanically generated signals compare favorably with analogous theoretical and experimental results for the AN/SQS-23. The mechanical device will be used with the Applied Research Laboratories scale model of the USS SKIPJACK (SSN 585) to evaluate the utility of RDT for ASW classification.

TABLE OF CONTENTS

	Page
ABSTRACT	iii
LIST OF FIGURES	vii
I. INTRODUCTION	1
II. DESCRIPTION OF THE MECHANICAL SIMULATOR	3
III. MEASUREMENTS	9
IV. CONCLUSIONS	19
APPENDIX: Electrical Power Requirements	21

LIST OF FIGURES

Figure No.	Title	Page
1.	Assembly Photographs of the Mechanical RDT Simulator	3
2.	Directivity Patterns for the 110 kHz Element	4
3.	Mechanically Generated Scaled 30 msec RDT Pulse	10
4.	Time-Pressure Envelope and Instantaneous Frequency Function; Scaled 30 msec RDT Pulse	11
5.	Analytically Derived Time-Pressure Envelope and Instantaneous Frequency Function; 30 msec RDT Pulse; Rotating Barrel Transducer	13
6.	Analytically Derived Time-Pressure Envelope and Instantaneous Frequency Function; 30 msec RDT Pulse; AN/SQS-23	14
7.	Time-Pressure Envelope and Instantaneous Frequency Function; AN/SQS-23; 30 msec RDT Pulse	15
8.	Time-Pressure Envelope and Instantaneous Frequency Function; Scaled 120 msec RDT Pulse	16
A.1	Power Consumed by a 0.25 hp Motor While Turning a 7 in., a 5 in., and a 5.25 in. Sphere in Water	22

I. INTRODUCTION

This memorandum describes the construction and performance of a device for mechanically simulating the Rotating Directional Transmission (RDT) mode of the AN/SQS-23. The device will be used with the Applied Research Laboratories (ARL) scale model of the USS SKIPJACK (SSN 585) to evaluate the utility of RDT for ASW classification. An analysis of the AN/SQS-23 RDT mode was performed by Grace and Bolch.* Their work includes a theoretical analysis of a mechanically rotating barrel transducer. Performance of the mechanical simulator described herein will be evaluated by comparison with Grace and Bolch's results.

---

*O. D. Grace and H. D. Bolch, "Simulation of the Acoustic Transmissions of the AN/SQS-23 Sonar System," Defense Research Laboratory Technical Report No. 68-7 (DRL-TR-68-7), 19 February 1968, p. 87.

II. DESCRIPTION OF THE MECHANICAL SIMULATOR

Construction and assembly of the mechanically rotated transducer are shown in Fig. 1. For versatility in use, two radiating elements, with resonant frequencies one octave apart, were included. The first element, shown in Fig. 1(a), is resonant at 110 kHz, with a scale factor of 22 (re 5 kHz, the frequency of the AN/SQS-23). The second element, shown in Fig. 1(b), is resonant at 220 kHz; the scale factor is 44.

A spherical shape was selected for the transducer housing. Noise and vibration measurements were performed on solid metallic prototype spheres. A standard hydrophone was located 6 ft from the sphere. Mechanical noise, and noise caused by turbulence in the fluid surrounding the sphere, were below receiver system noise at all rotating speeds. The window portion of the spherical housing was formed of a polyester resin--Scotchcast No. 2--poured in layers, then machined. The end caps were machined from brass. The interior spaces of the sphere are filled with castor oil.

The specified beamwidth of the AN/SQS-23 is 10 deg at the half power points, with first minor lobe suppression of 13 dB. Both the 110 kHz and 220 kHz elements were formed to meet these specifications. The directivity pattern for the 110 kHz element with a plane face window is shown as the solid curve in Fig. 2. The beamwidth is 8 deg (-3 dB), with 14 dB first minor lobe suppression. When this element was placed in the spherical window of the simulator, the directivity pattern shown by the broken curve in Fig. 2 was measured. The

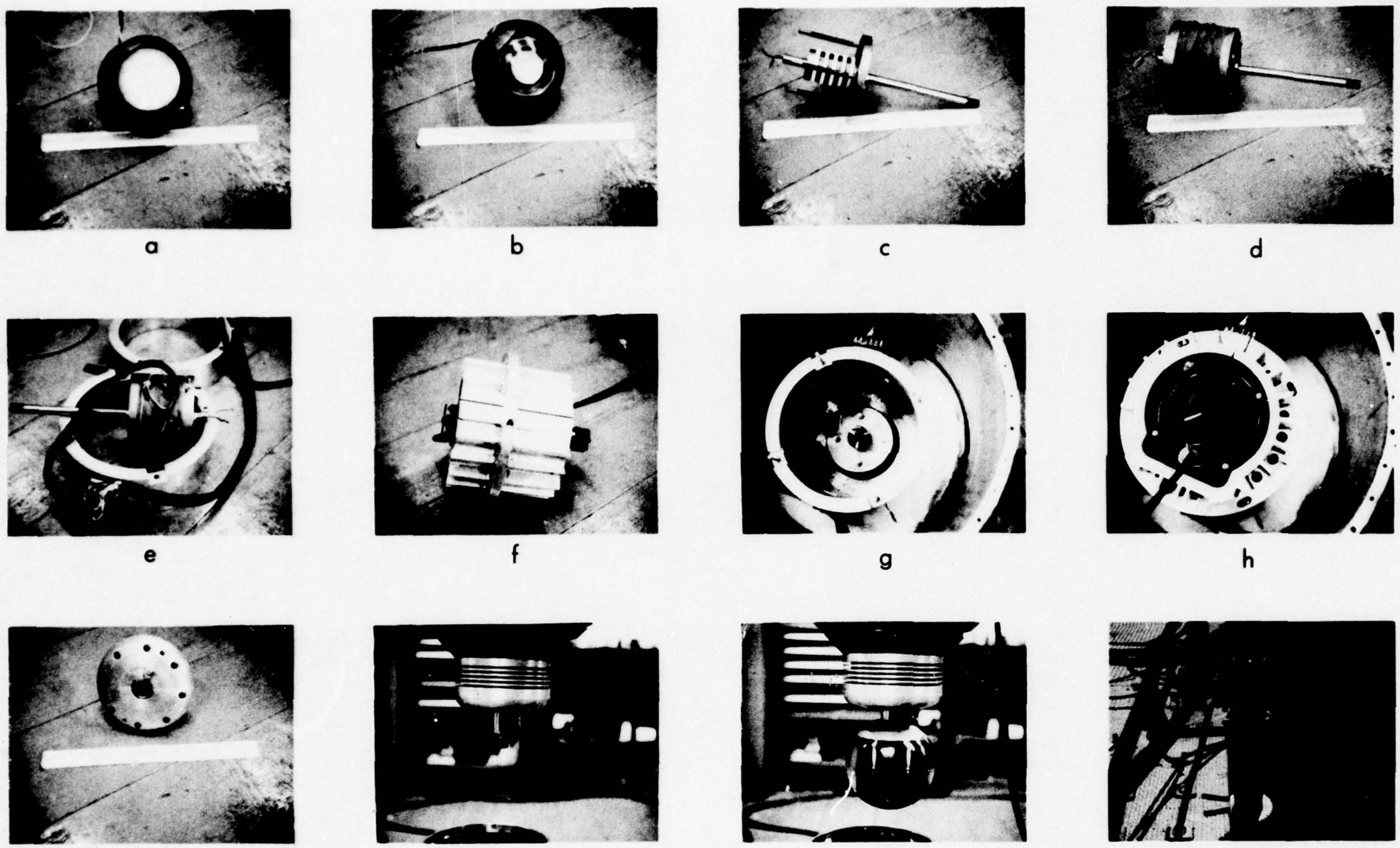

FIGURE 1
ASSEMBLY PHOTOGRAPHS OF THE MECHANICAL RDT SIMULATOR

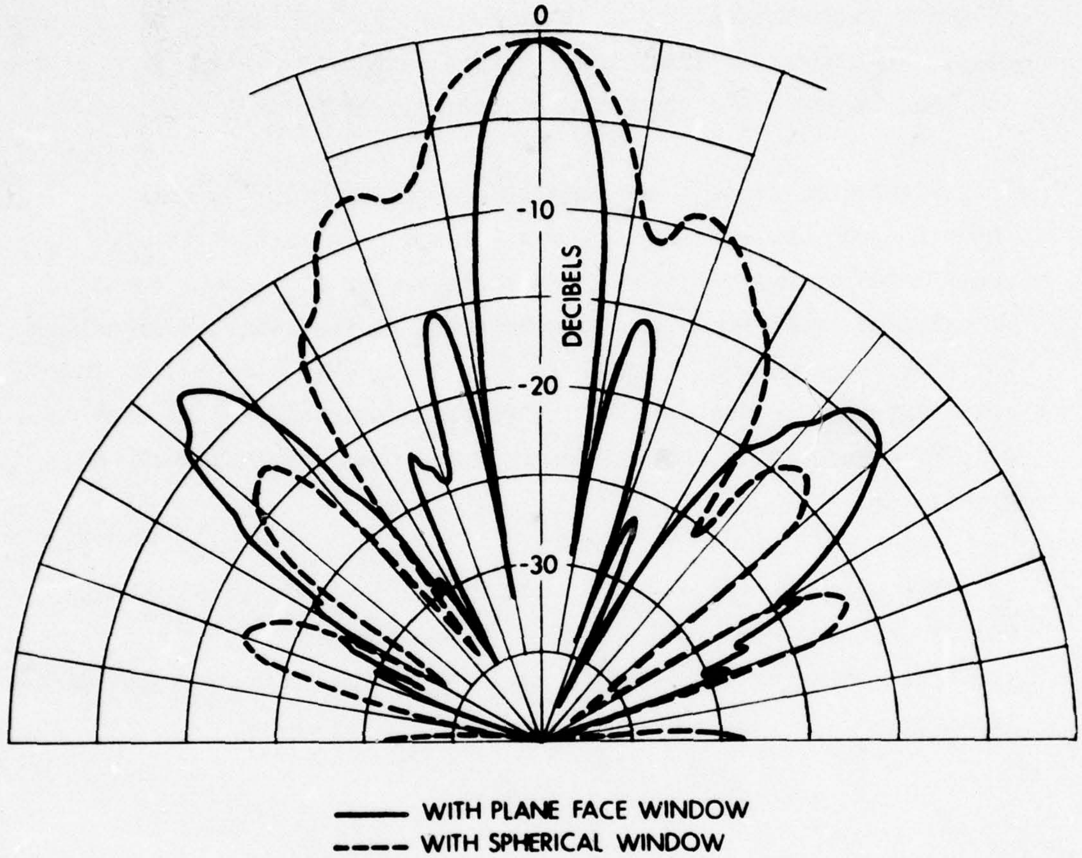

FIGURE 2
DIRECTIVITY PATTERNS FOR THE 110 kHz ELEMENT

ARL - UT
AS-69-1081
KJD - WDB
9-26-69

beamwidth is 16 deg (-3 dB), with 8 dB minor lobe suppression. Sound velocity in Scotchcast No. 2 is approximately 1.7 times that in water (i.e., 2490 m/sec). Thus, the spherical window is acting as a diverging lens to yield the change in directivity shown in Fig. 2.

Electrical signals are coupled to the radiating elements through carbon brushes on copper sliprings. Two diametrically positioned brushes per ring are used to insure continuous contact. To date, no brush noise has been detected in the radiated signals. The slipring assembly is shown in Fig. 1(c), (d), and (e). A fourth split slipring is included in the slipring assembly and is used as a switch to generate a time reference pulse each revolution of the transducer.

The pulse length of a rotating transmission is determined by the beamwidth of the radiation, and its rotational velocity. For a specified duration, T, with a beamwidth, B, the velocity required is given by

$$V_{(rpm)} = \frac{B}{T} \cdot \frac{60}{360} \quad ,$$

where B is measured in degrees, and T is specified in seconds. Scaled durations of the AN/SQS-23 Short Pulse (SP), Medium Pulse (MP), and Long Pulse (LP) transmissions are: 0.091 msec, 1.36 msec, and 5.45 msec, respectively (1/22 scale factor). The associated rotational velocities are, then: SP - 29,000 rpm; MP - 1960 rpm; LP - 490 rpm. The scaled SP velocity cannot be achieved with the device described herein.

The drive motor assembly is shown in Fig. 1(f), (g), and (h). The spherical housing with the radiating elements is attached directly to the motor shaft. The motor shaft passes through a loosely fitted O-ring water seal, shown in Fig. 1(i) and 1(j). The seal housing is filled with oil under slight pressure to oppose water leakage around

the shaft. The electrical power required to rotate the prototype and transducer spheres, with and without the water seal(s), is described in the Appendix.

A close-up view of the assembled simulator is shown in Fig. 1(k). Figure 1(l) shows the above water parts of the device in place at the Lake Travis Test Station (LTTS) of ARL.

III. MEASUREMENTS

Measurements were performed at the LTTS. Figure 3 is an oscilloscope photograph of a mechanically generated scaled 30 msec RDT pulse. The driving frequency was 110 kHz. Side lobe suppression is 9.5 dB. The pulse appearing 1.8 major scale divisions after the main lobe of the transmission is a reflection from a nearby transducer support column.

The analog signals were recorded on magnetic tape and were analog-to-digital converted for computation of the instantaneous frequency function(s). The instantaneous frequency of a signal is the time derivative of the signal phase. That is,

$$\hat{f}_i = \frac{d\varphi_i}{dt} = 2\pi \left\{ f_o - \frac{f_o}{2\pi} \left[\frac{X_i\left(Y_{i+1}-Y_i\right) - Y_i\left(X_{i+1}-X_i\right)}{X_i^2 + Y_i^2} \right] \right\} ,$$

where

$\hat{f}_i$ = instantaneous frequency,

φ_i = signal phase,

i = sample index number = 1, 2, 3,..., n,

f_o = driving frequency,

X_i, Y_i = quadrature components of the digital signal.

The time-pressure envelope and instantaneous frequency function for the pulse shown in Fig. 3 are plotted in Fig. 4. These results are to be compared with analogous results from Grace and Bolch, as

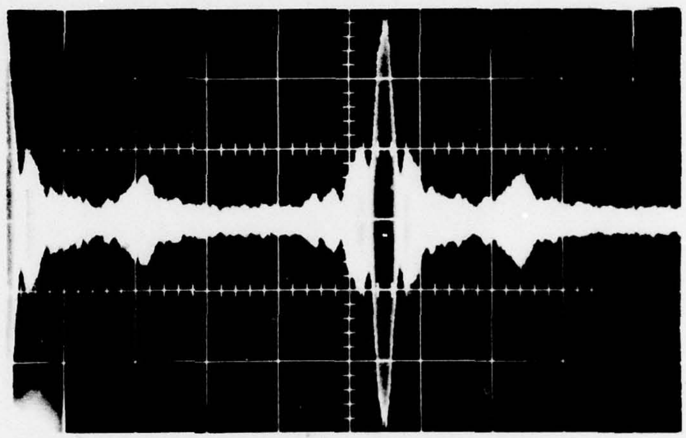

FIGURE 3
MECHANICALLY GENERATED SCALED 30 msec RDT PULSE
$f_0 = 110$ kHz
SCALE: 5 msec/div

ARL - UT
AS-69-1090
WWR - EJW
9 - 19 - 69

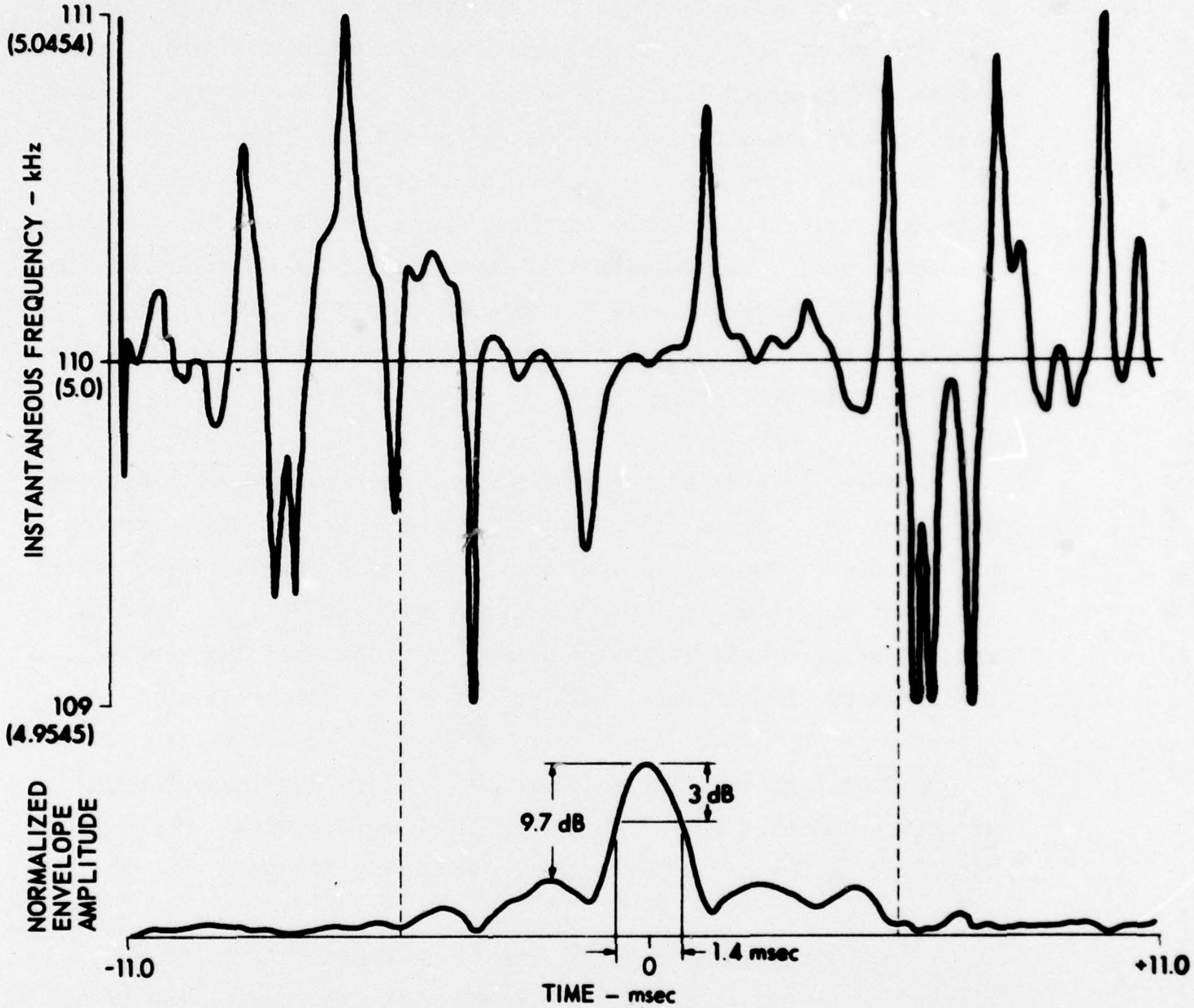

FIGURE 4
TIME-PRESSURE ENVELOPE AND INSTANTANEOUS FREQUENCY FUNCTION
SCALED 30 msec RDT PULSE f_0 = 110 kHz
SCALE FACTOR: 22

ARL - UT
AS-69-686
WWR - RFO
7 - 16 - 69

presented in Figs. 5 through 7. Figure 5 shows the analytically derived time-pressure envelope and instantaneous frequency function for a 30 msec RDT pulse generated by rotating a barrel transducer. Only the major lobe and first time minor lobes of the pulse are shown. First minor lobe suppression is 11.5 dB. Note the Doppler evidenced by the slope of the "baseline" of the frequency function. The frequency excursions occurring at the nulls of the pressure envelope reflect the change of phase which occurs as the beam passes through a null. The magnitude of an excursion is a measure of the depth of the null--i.e., of the rate of change of phase. The (instantaneous) energy radiated at these (instantaneous) frequency excursions is negligible.

Figure 6 is the analogous results for an analytically derived AN/SQS-23 RDT. First minor lobe suppression is 14.8 dB. There is no Doppler evident in the frequency function. The direction of the frequency excursions is opposite those shown in Fig. 5. This is a manifestation of the different manner in which the beam is formed and rotated. Effectively, this difference is inconsequential.

Figure 7 shows the time-pressure envelope and instantaneous frequency function for an AN/SQS-23 30 msec RDT pulse. There is little or no Doppler evident in the frequency function.

Qualitatively the results from the mechanical simulator, presented in Fig. 4, compare favorably with the results for the AN/SQS-23 presented in Figs. 5 through 7 (the analogous time-frame, major lobe and first two minor lobes, is delineated in Fig. 4 by the vertical broken lines). There is no evidence of Doppler in the frequency function for the mechanical simulator shown in Fig. 4.

Figure 8 is the time-pressure envelope and instantaneous frequency function for a mechanically simulated scaled 120 msec RDT pulse. The indicated minor lobe suppression is nominally 4 dB less

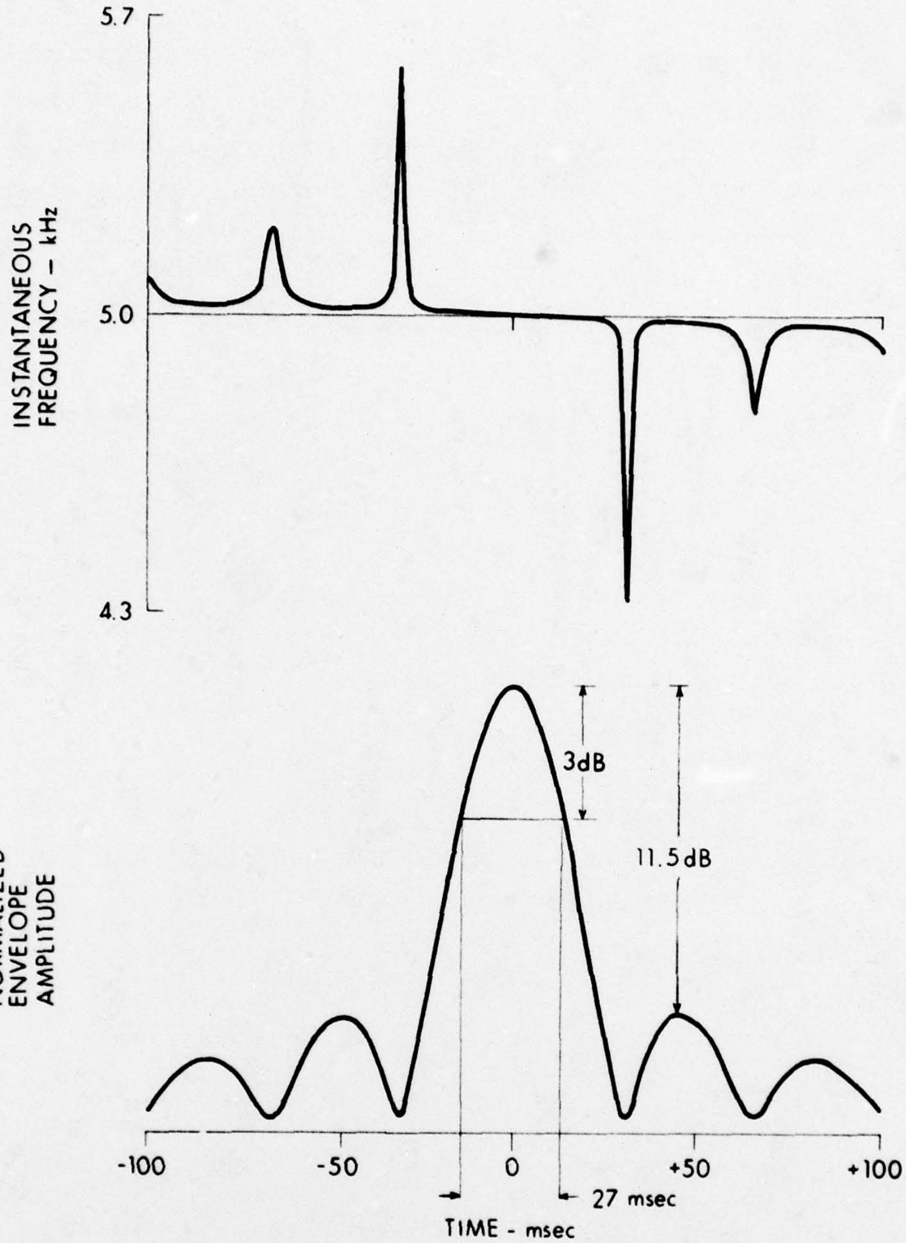

FIGURE 5
ANALYTICALLY DERIVED TIME-PRESSURE ENVELOPE AND INSTANTANEOUS FREQUENCY FUNCTION
30 msec RDT PULSE $f_0 = 5$ kHz
ROTATING BARREL TRANSDUCER
(FROM GRACE AND BOLCH)

ARL - UT
AS-69-1082
KJD - WDB
9-26-69

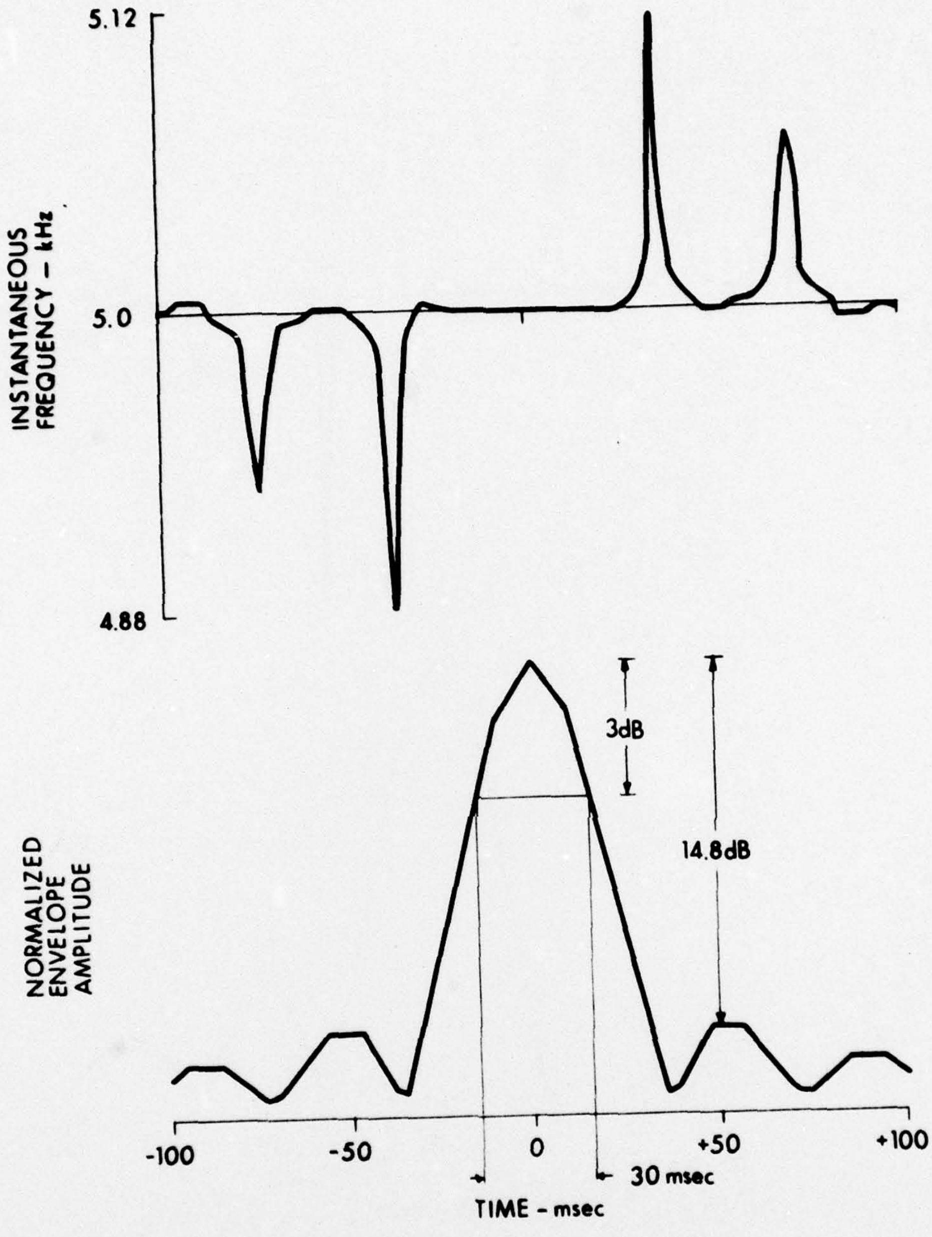

FIGURE 6

ANALYTICALLY DERIVED TIME-PRESSURE ENVELOPE AND INSTANTANEOUS FREQUENCY FUNCTION

30 msec RDT PULSE f_0 = 5 kHz

AN/SQS-23

(FROM GRACE AND BOLCH)

ARL - UT
AS-69-1083
KJD - WDB
9-26-69

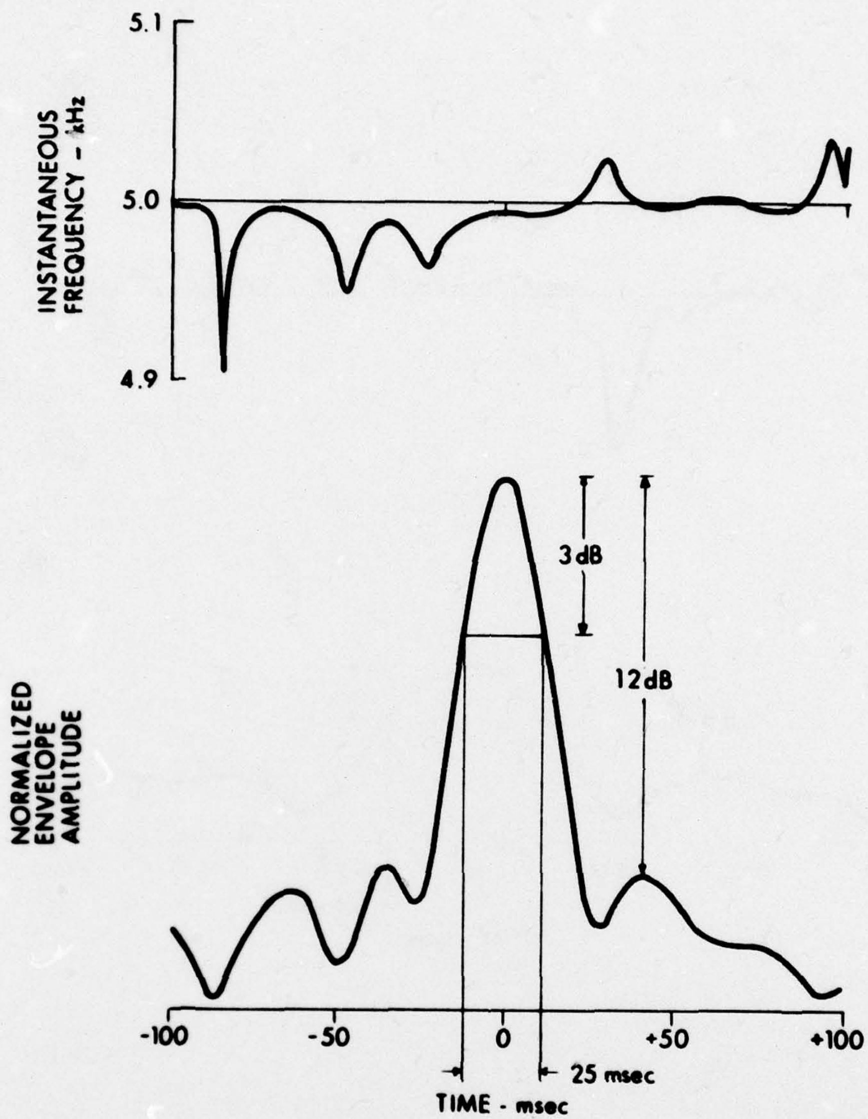

FIGURE 7

TIME - PRESSURE ENVELOPE
AND INSTANTANEOUS FREQUENCY FUNCTION
AN/SQS - 23
30 msec RDT PULSE f_0 = 5 kHz
(FROM GRACE AND BOLCH)

ARL - UT
AS-69-1084
KJD - WDB
9-26-69

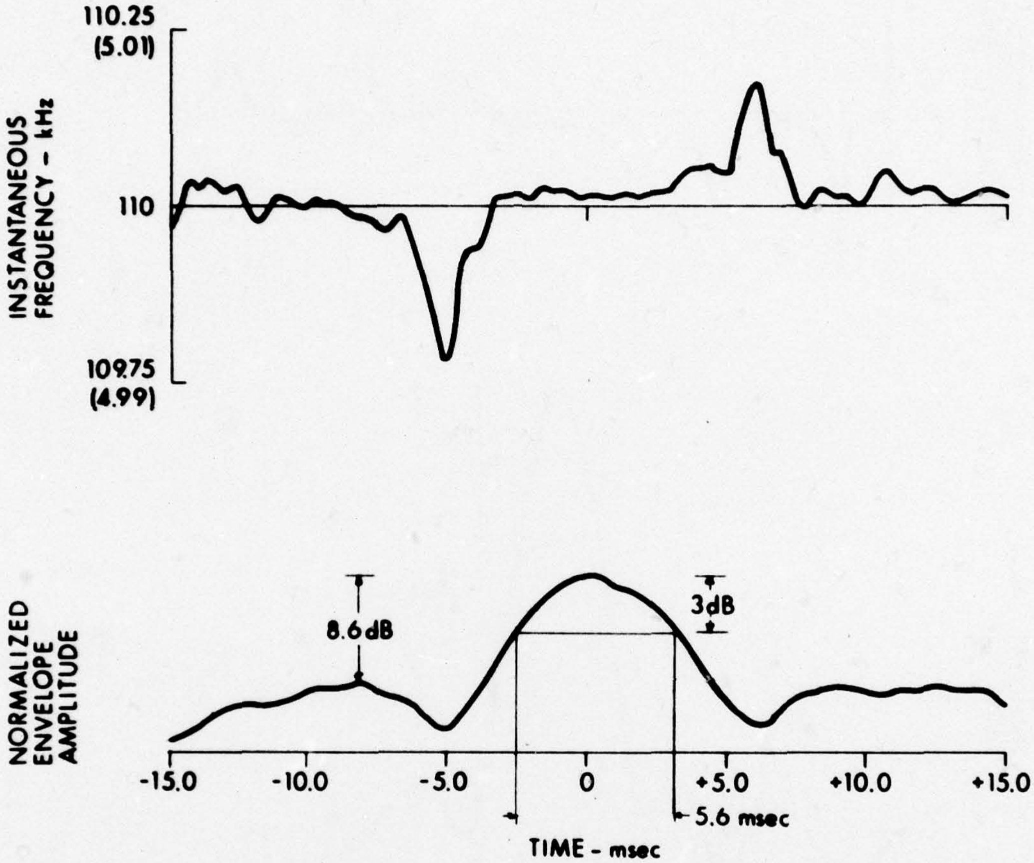

FIGURE 8

TIME - PRESSURE ENVELOPE
AND INSTANTANEOUS FREQUENCY FUNCTION
SCALED 120 msec RDT PULSE f_0 = 110 kHz
SCALE FACTOR: 22

ARL - UT
AS-69-1085
KJD - WDB
9-26-69

than that predicted by Grace and Bolch for this duration for a rotating barrel transducer. The magnitude and direction of the frequency excursions are comparable to those predicted for the AN/SQS-23. Results for a 120 msec AN/SQS-23 RDT were not reported by Grace and Bolch.

IV. CONCLUSIONS

The mechanical device described herein for simulating the rotating directional transmissions of the AN/SQS-23 uses a circular piston transducer mounted in a (rotatable) spherical housing formed of a material with suitable acoustic properties. The use of a thick spherical face window alters the radiation pattern of the transducer from what it would be when the element is enclosed by a plane face window of the same material. That is, the major lobe is broadened and the minor lobes are raised. It was concluded that these changes were caused by the spherical window acting as a diverging lens.

The time-pressure envelopes and instantaneous frequency functions of scaled 30 msec and 120 msec RDT pulses generated by the mechanical simulator compare favorably in form and magnitude with analogous full-scale AN/SQS-23 waveforms. It is concluded that mechanical generation yields realistic simulations of rotating directional transmissions. Hence, the mechanical simulator will be used with the ARL SKIPJACK model to evaluate the utility of RDT for ASW classification.

APPENDIX

Electrical Power Requirements

The rotating spherical transducer housing is attached to the output shaft of a 0.25 hp variable speed dc motor. Initial noise and vibration measurements were performed using 5 in. o.d. and 7 in. o.d. solid aluminum spheres (the diameter of the transducer housing is 5.25 in.). Motor input power was monitored during all tests. Figure A-1 displays the results of these measurements. The abscissa is rotational speed in rpm. The ordinate is electrical power consumed in watts. Rated motor power (186 W) is indicated by the horizontal solid line. Two curves each are plotted for the 5 in. diam aluminum sphere (X's) and the 7 in. diam aluminum sphere (open circles). The upper curve of each set was obtained with the O-ring water seal (Fig. 1(i), (j), and (k)) in place and immersed. The lower curve of each set was obtained with the O-ring seal removed and only the sphere immersed. It is obvious that frictional forces within the O-ring seal constituted a significant load on the motor. The curve for the spherical transducer housing (open triangles) was obtained with the O-ring seal in place and lubricated by an oil bath. This curve deviates from the lower curve for the 5 in. aluminum sphere (without O-ring seal) at the higher rotational speeds and probably indicates inadequate lubrication of the O-rings due to too low pressure in the oil bath.

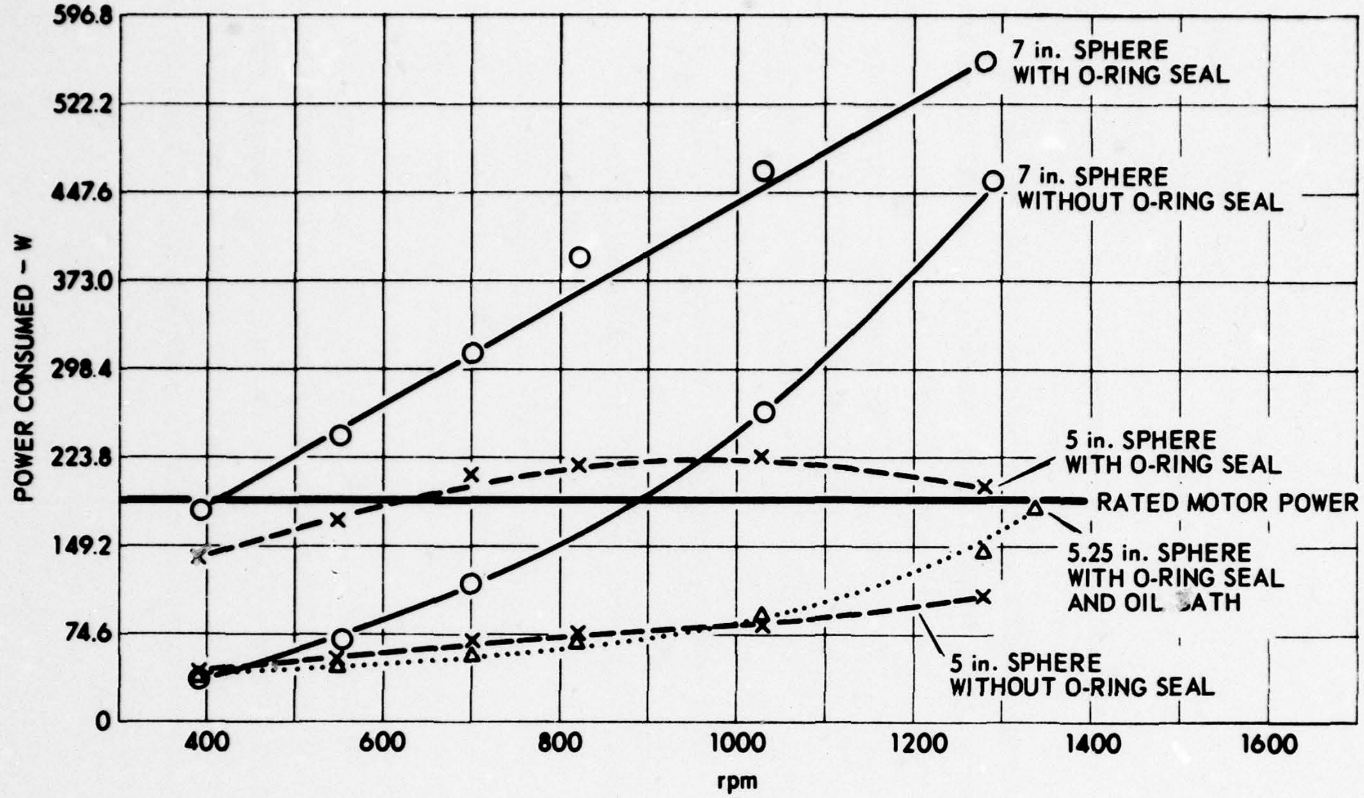

FIGURE A-1
POWER CONSUMED BY A 0.25 hp MOTOR WHILE
TURNING A 7 in., A 5 in., AND A 5.25 in. SPHERE IN WATER

ARL - UT
AS-69-695
WWR - RFO
7 - 17 - 69

17 October 1969

DISTRIBUTION LIST FOR
ARL-TM-69-18
UNDER CONTRACT N00024-69-C-1129
UNCLASSIFIED-FOUO

Copy No.	
1 - 2	Commander, Naval Ship Systems Command Department of the Navy Washington, D. C. 20360 Attn: SHIPS OOV1C
	Commander Naval Undersea Research and Development Center San Diego Division 271 Catalina Boulevard San Diego, California 92152
3 - 4	Attn: Code D606
5	Bryson Pennoyer, Code D554
6	Mr. Littrell, Code 603
7	Dr. Watson, Code 556
8	Library
9	Commanding Officer and Director U. S. Navy Underwater Sound Laboratory Fort Trumbull New London, Connecticut 06320 Attn: Code 2242
10	Director U. S. Naval Personnel Research Activity Department of the Navy San Diego, California 92152
11	Office of Naval Research Resident Representative The University of Texas at Austin 2507 Main Building Austin, Texas 78712

Dist. List for ARL-TM-69-18 under Contract N00024-69-C-1129 (Cont'd)

Copy No.	
12	Computer Science Division, ARL/UT
13	Signal Physics Division, ARL/UT
14	K. J. Diercks, ARL/UT
15	R. K. Goodnow, ARL/UT
16	W. D. Howard, ARL/UT
17	S. P. Pitt, ARL/UT
18	W. W. Ryan, ARL/UT
19	J. K. Vaughan, ARL/UT
20	R. H. Wallace, ARL/UT
21	Library, ARL/UT

APPLIED
RESEARCH
LABORATORIES
THE UNIVERSITY OF TEXAS
AT AUSTIN

~~For Official Use Only~~